The Astrophysical Journal, 929:17 (6pp), 2022 April 10 https://doi.org/10.3847/1538-4357/ac54b9

The Accurate Mass Distribution of M87, the Giant Galaxy with Imaged Shadow of Its Supermassive Black Hole, as a Portal to New Physics

Mariafelicia De Laurentis[1,2] and Paolo Salucci[3,4]
[1] Dipartimento di Fisica "E. Pancini," Universitá di Napoli "Federico II," Complesso Universitario di Monte S. Angelo, Edificio G, Via Cinthia, I-80126 Napoli, Italy; mariafelicia.delaurentis@unina.it
[2] INFN Sez. di Napoli, Complesso Universitario di Monte S. Angelo, Edificio G, Via Cinthia, I-80126 Napoli, Italy
[3] SISSA International School for Advanced Studies, Via Bonomea 265, I-34136, Trieste, Italy; salucci@sissa.it
[4] INFN, Sezione di Trieste, Via Valerio 2, I-34127, Trieste, Italy
Received 2021 May 5; revised 2022 January 15; accepted 2022 January 25; published 2022 April 8

Abstract

The very careful Event Horizon Telescope estimate of the mass of the supermassive black hole at the center of the giant cD galaxy M87, allied with recent high-quality photometric and spectroscopic measurements, yields a proper dark/luminous mass decomposition from the galaxy center to its virial radius. That provides us with decisive information on crucial cosmological and astrophysical issues. The dark and the standard matter distributions in a wide first time detected galaxy region under the supermassive black hole gravitational control. The well-known supermassive black hole mass versus stellar dispersion velocity relationship at the highest galaxy masses implies an exotic growth of the former. This may be the first case in which one can argue that the supermassive black hole mass growth was also contributed by the dark matter component. A huge dark matter halo core in a galaxy with inefficient baryonic feedback is present and consequently constrains the nature of the dark halo particles. The unexplained entanglement between dark/luminous structural properties, already emerged in disk systems, also appears.

Unified Astronomy Thesaurus concepts: Dark matter distribution (356); Supermassive black holes (1663); Dark matter (353)

1. Introduction

The distribution of dark matter (DM) in galaxies is extremely relevant for cosmology and particle physics. Let us sketch the state of the art: the well-known Λ cold dark matter (CDM) scenario, employing cosmological n-body simulations, predicts that the DM halo density, in any virialized object, follows the Navarro–Frenk–White (NFW) profile (Navarro et al. 1996), characterized by a central cusp $\rho(r) \propto r^{-1}(r + r_s)^{-2}$ with r_s length scale depending on the value of the halo mass. However, the individual and coadded kinematics of spirals, low surface brightness (LSB) galaxies, and dwarf irregulars clearly show that the main baryonic component, a stellar disk of surface density[5] (Freeman 1970),

$$\Sigma_\star(r) = \frac{M_D}{2\pi R_D^2} e^{-r/R_D}, \quad (1)$$

is embedded in a dark halo with a cored density distribution (de Blok 2010; Karukes & Salucci 2016; Salucci 2018, 2019): $\rho(r) \propto (r_0 + r)^{-1}(r_0^2 + r^2)^{-1}$. The above discrepancy between the empirical profile and the Λ CDM n-body outcome simulation is particularly strong in dwarfs and low luminosity disk systems (Karukes & Salucci 2016). Remarkably, after a proper circular velocity decomposition into its dark and luminous components, all disk systems of stellar masses $5 \times 10^7 M_\odot \leqslant M_\star \leqslant 3 \times 10^{11} M_\odot$ show a cored dark halo density profile (see also de Martino et al. 2020). This is also shown by coadded studies of rotation curves (Salucci 2007; Salucci et al. 2007; Dehghani et al. 2020) (see also Di Paolo 2021, online lecture[6]. At high redshifts the situation is open although some evidence for dark matter cores is appearing (Salucci et al. 2021). However, it is worth noting that supernovae explosions in stellar disks may originate "baryonic feedback" capable of fabricating the observed DM cores from the original cusps (Di Cintio et al. 2014). In these systems, however, another "anomaly" is still unexplained: the structural parameters of the mass distribution, i.e., ρ_0, r_0, and the disk mass and length scale M_D, R_D, are surprisingly very well correlated among themselves (Salucci 2019).

The above discussion introduces the primary goal of this work: to derive the mass distribution of the luminous and dark components of M87. This massive cD elliptical galaxy, located at the center of the Virgo Cluster, is the biggest one in the universe within a radius of 0.5 Gpc. In detail: its stellar spheroid mass is 20 times bigger than that of the disk of our Galaxy, while its dark halo mass is 100 times more massive. We will then investigate the galaxy structural properties in an extreme object.

Moreover, as any spheroidal galaxy, M87 has, at its center, a very supermassive black hole (SMBH); its mass estimates, obtained from different methods/measurements, have ranged from $(3.5 \pm 0.8) \times 10^9 M_\odot$ to $7.22^{+0.34}_{-0.40} \times 10^9 M_\odot$ (Walsh et al. 2013; Oldham & Auger 2016). This SMBH is the first and the only one so far to be imaged (as of 2019 April; Akiyama et al. 2019a, 2019b). The image shows its shadow, surrounded by an

[5] The size of the stellar disk is defined as $R_{\rm opt} \equiv 3.2\, R_D$.

[6] https://www.youtube.com/playlist?list=PLe9EzUPIhHubf_m-F7eK10t7A4MIg4fIu

asymmetric emission ring with a diameter of 3.36×10^{-3} pc (0.01 lt-yr). This result has a consequence for the present work: as a by-product, the Event Horizon Telescope (EHT) has finely measured the SMBH mass: $(6.5 \pm 0.2_{\rm stat} \pm 0.7_{\rm sys}) \times 10^9 M_\odot$ (Akiyama et al. 2019b). Its value and small uncertainty play an essential role in the present work's results. Finally, we assume for M87 the EHT distance of 16.5 Mpc (Akiyama et al. 2019a).

This work is organized as follows. In Section 2, we describe the method obtained to derive the M87 mass model accurately. In Section 3, we investigate the properties of the central SMBH and of the other mass components of this giant galaxy. In the conclusions, Section 4, we summarize our findings specifying how M87 serves as a cosmic laboratory for many unsolved mysteries of the universe.

2. Method: Deriving the Mass Distribution in M87

The giant elliptical M87 is home to several different dynamical populations as planetary nebulae, globular clusters, and satellite galaxies. They can be used as multiple, independent, and well-extended tracers of galactic gravitational fields (see, e.g., Schuberth et al. 2010; Agnello et al. 2014; Napolitano et al. 2014; Salucci 2019). This wealth of data, alongside high-resolution photometry and spectroscopy, also allows careful mass modeling because, in this object, we can assume a spherical symmetry in all the mass components. The mass structure of M87 has been the subject of many studies (Murphy et al. 2011; Strader et al. 2011; Zhu et al. 2014). Recently, a substantial improvement in the determination of its gravitational potential has been obtained by Oldham & Auger (2016a) for a region extending from very near to the center out to the virial radius.

In relation to the galaxy DM halo density profile, they adopted four models (Oldham & Auger 2016a): one cusped (the well-known NFW profile; Navarro et al. 1996) and three cored (the LOG, the gNFW, and the cgNFW ones). They found that the mass model with the DM cored profiles fared better in fitting the observational data than the cuspy ones (Navarro et al. 1996). However, the aforementioned cored profiles raise doubts that they can describe the DM distribution in galaxies in a physically correct way. In fact, the LOG profile, introduced in the universal rotation curve of spirals (Persic et al. 1996), holds only out to their optical radii, outside which kinematical and weak lensing data strongly favor the Burkert profile (Salucci et al. 2000; Gentile et al. 2007; Salucci 2019), which declines with radius in the outermost halo regions (e.g., Gentile et al. 2007), while the LOG profile flattens there. The gNFW profile features an NFW profile with the addition of a core,

$$\rho(r) = \frac{\rho_0}{\left(\frac{r}{r_s}\right)^{\alpha}\left(1+\frac{r}{r_s}\right)^{3-\alpha}},$$

with α as the inner slope and $x = r/r_s$ with r_s length scale. However, this generalization of the NFW profile not only leads to multiple degeneracies (Klypin et al. 2001) but also increases, by one, the number of halo parameters, with no physical justification. In fact, in both simulations and observations, the resulting DM density profiles have just two free parameters (a halo density and a halo length scale) and seem to not require a third. Actually, in the above investigations, one finds a tight relationship connecting the two, reducing the number of necessary parameters to just one (Salucci 2019). Finally, at large radii, this density profile does not necessarily converge to the NFW one. Similar arguments hold for the cgNFW profile also used in Oldham & Auger (2016a), which has two free parameters more than the NFW one.

Remarkably, in spirals, LSBs, dwarf irregulars, dwarf spheroidals, and also ellipticals, the Burkert DM halo profile (not considered in Oldham & Auger 2016a) alongside with its luminous counterparts fits all the available kinematics, including individual and coadded rotation curves (RCs) excellently (Salucci 2019). Therefore, in this work, we adopt the latter profile and so we can also compare its dark structure with that of galaxies of different Hubble types and halo mass.

The study by Oldham & Auger (2016a) has derived the total mass distribution of M87 up to its virial radius at 1.3 Mpc. The stellar photometry, available out to 210 kpc, in Oldham & Auger (2016b), shows a 2D light distribution which is very different from the Sérsic profile, generally found in ellipticals. We have an extended envelope, outside the inner stellar core, likely due to the fact that the M87 spheroid has been formed by the first burst of star formation, followed by a continuous infall of luminous matter lasting several Gyrs. The Nuker profile best models the surface luminosity profile of the stellar spheroid

$$I(R) = I_0\left(\frac{R}{R_b}\right)^{-\zeta}\left(1+\left[\frac{R}{R_b}\right]^{\alpha}\right)^{\frac{\zeta-\eta}{\alpha}}, \quad (2)$$

where, by following Oldham & Auger (2016b), we have $I_0 = 3.5 \times 10^9\, L_\odot\ \mathrm{kpc}^{-2}$, $\zeta = 0.186$, $\eta = 1.88$, $r_b = 1.05$ kpc, and $\alpha = 1.27$. Moreover, in M87, $M_B = -20.5$, and the half-light radius reaches the value of $r_e = (73.5 \pm 7)$. It is important to remark that Equation (2) provides us with an accurate stellar mass distribution also in the region 1 kpc $< r <$ 5 kpc, neighboring the central SMBH. From Equation (2) we derive the corresponding M87 disk scale length R_D in the following way: in spirals, R_D is the radius inside which the fraction of light is 0.2 times the total one, so we get $R_D^{\rm M87} = 10 \pm 1$ kpc. This galaxy has one of the largest half-light radii within the region-wide 1 Gpc^3 of the universe. However, the value of $R_D^{\rm M87}$ is in line with that of the most massive spirals. One can argue that the peculiarity in the M87 stellar distribution emerges only at $r > 50$ kpc, where the dark matter largely dominates the total mass distribution.

The mass profile of the luminous component is obtained from Equation (2) by means of

$$M_\star(r) = -\left(\frac{M_{\rm sph}}{L_B}\right)\int_0^r r^2\left(\int_r^\infty \left(\frac{dI(R)}{dR}\right)\frac{dR}{\sqrt{R^2-r^2}}\right)dr. \quad (3)$$

This profile has just one free parameter: $M_{\rm sph}$ the spheroid mass.

The gravitating mass profile $M(r)$ that we use in this work was obtained from the Jeans method applied to the kinematics of different tracers of the gravitational field which assure 11 M87 independent data points (see Oldham & Auger 2016a). They have derived the mass profile $M(r)$ for the case of spherical symmetry and also found that possible kinematical anisotropies induce only a moderate effect in the mass profile. In fact, by varying the anisotropy content, the corresponding mass profiles $\log M(r)$ results are all very similar and lie, at any radius r, within 0.2 dex from the isotropic solution (Oldham & Auger 2016a) (see Figure 1). It is worth noting that these uncertainties in $\log M(r)$ are much smaller than the range of the measured $\log M(r)$ masses, that is 2.5 dex; this opportunity is very rare for spheroidal galaxies. Therefore, in this work, we will adopt the isotropic

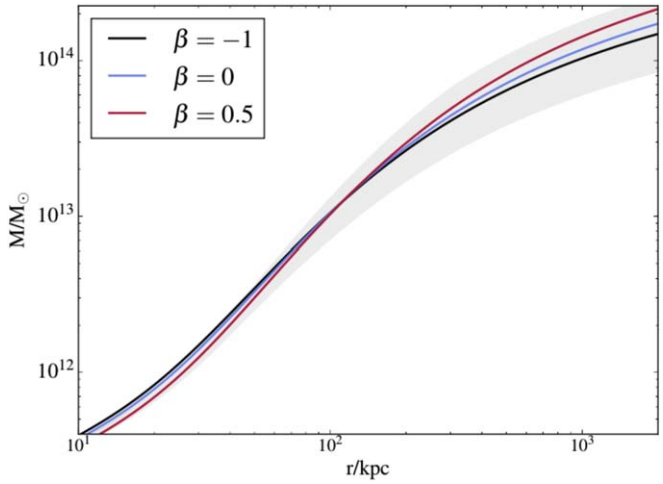

Figure 1. The mass profile of the total mass of M87. β is the standard anisotropy parameter (see Oldham & Auger 2016a).

profile $\log M(r)$ of Oldham & Auger (2016a) to represent the gravitating mass profile of M87, and we consider the effect of kinematical anisotropies by assigning a 0.2 dex uncertainty to the log mass measurements.

For DM, we adopt the Burkert profile; this choice is the only difference concerning the modeling in Oldham & Auger (2016a), but it is very substantial and, in addition, can also affect the resulting value of the mass of the luminous spheroid. Then,

$$\rho_h(r) = \frac{\rho_0 r_0^3}{(r + r_0)(r^2 + r_0^2)}, \tag{4}$$

where the core radius r_0 and the central density ρ_0 are the free parameters of the model. As a result,

$$M_h(r) = M_0 \left[\log\left(1 + \frac{r}{r_0}\right) - \tan^{-1}\left(\frac{r}{r_0}\right) + \frac{1}{2}\log\left(1 + \left(\frac{r}{r_0}\right)^2\right)\right], \tag{5}$$

where $M_0 = 6.4\rho_0\, r_0^3$. Let us notice that, in the *global mass modeling* of such a giant galaxy of about $10^{14} M_\odot$, the EHT value for the central black hole mass ($(6.5 \pm 0.2_{\rm stat} \pm 0.7_{\rm sys}) \times 10^9 M_\odot$) shows that the latter does not play any gravitational role (different is the situation in the innermost kiloparsecs, discussed below). Therefore, the mass model, with its three free parameters, reads as:

$$M_{\rm mod}(r;\, M_{\rm sph},\, r_0,\, \rho_0) = M_\star(r;\, M_{\rm sph}) + M_h(r;\, r_0,\, \rho_0). \tag{6}$$

Then, we proceed using the standard χ^2 fitting the 11 independent data of the mass profile $M(r)$ with the mass model of Equation (6) and obtaining so the three free parameters and the related triangular plots yield their statistical uncertainties. It is evident in Figure 2 that the adopted DM profile allied with a much smaller contribution from the stellar spheroid reproduces the distribution of the gravitating mass of the galaxy. Therefore, the mass model can be written as $M_{\rm mod}(r;\, M_{\rm sph},\, \rho_0,\, r_0)|_{best\ fit}$. The resulting values of the

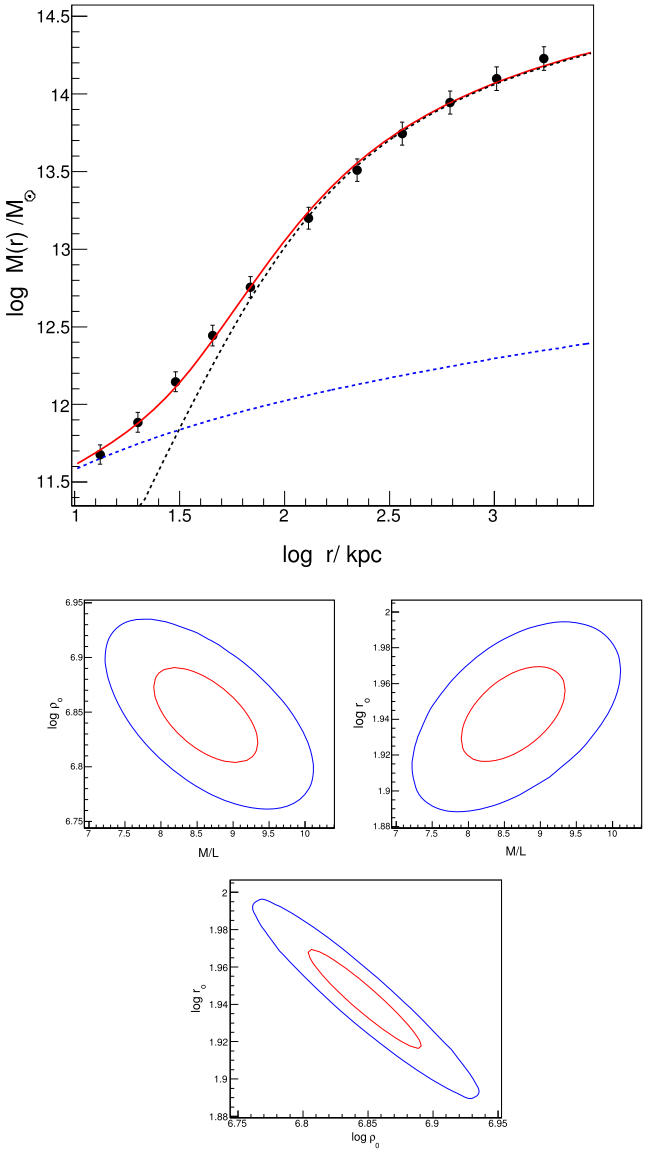

Figure 2. Top: the model mass distribution in M87 (red line). Also indicated: the stellar Nuker (dashed blue line) and the Burkert profiles (dashed black line). Bottom: the 1-sigma (red line) and 2-sigma (blue line) contour plots of the mass model free parameters.

best-fit parameters are $M_{\rm sph} = (1.3 \pm 0.1) \times 10^{12}\, M_\odot$ which leads to a mass-to-light ratio of $M_{\rm sph}/L_V = (8.6 \pm 1.2) M_\odot L_\odot^{-1}$, $r_0 = (91.2 \pm 9.0)$ kpc, and $\rho_0 = (4.7 \pm 0.9) \times 10^{-25}$ g cm^{-3}. The nominal value for the virial radius is $R_{200} = (1.3 \pm 0.2)$ Mpc; the halo mass within R_{200} is $M_{200}^{\rm M87} = (1.3 \pm 0.3) \times 10^{14} M_\odot$ and the luminous–dark mass ratio is about 10^{-2}. Therefore, M87 is one of the biggest galaxies in the universe at the upper end of the galaxy formation process. Noticeably, a particle situated at R_{200}, in rotation around the center of M87, would make a complete orbit in not less than 13 Gyr, the current age of the universe, a fact that might not be a coincidence.

Let us define, for this spherical pressure dominated object, a circular velocity analog to that of the rotationally dominated disk systems for which $V^2_{\rm M87,disk}(r) \equiv G\, M_{\rm M87,disk}(r)/r$ where $V_{\rm M87,disk}(r)$ is the circular velocity that allows a point mass, at a distance r from the center of any galaxy, to stay in rotational

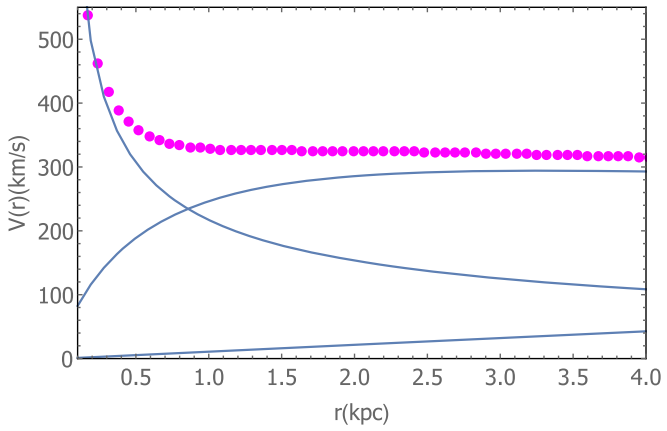

Figure 3. The analogous rotation curve in the innermost regions of M87 (magenta circles). The decreasing and rising curves are the SMBH and spheroid components. Note its flat behavior and the irrelevancy of the dark matter component (the lowest blue line).

equilibrium. Then, for M87, considering also Equations (3), (5), we have

$$GM(r)/r = V^2_{\rm M87}(r) = GM_{\rm mod}/r = V^2_{\rm mod}(r) = [V^2_{\rm SMBH}(r) + V^2_{\star}(r) + V^2_{h}(r)]_{\rm mod}. \quad (7)$$

Since the model fits the data very well, e.g., $M_{\rm mod}(r) \simeq M(r)$, we can accurately determine the velocity profile (see Figure 3). Moreover, $V(R_{\rm opt}) = \left(\frac{GM(R_{\rm opt})}{R_{\rm opt}}\right)^{1/2} = 360 \pm 5$ km s^{-1} and for a spherical and isotropic distribution we derive the dispersion velocity $\sigma(r_e)$ from $G^{-1}\, V^2(r_e) r_e = G^{-1} 3\sigma(r_e)^2\, r_e$ that yields $\sigma(r_e) = 358 \pm 5$ km s^{-1}.

Not unexpectedly, the DM density in the outer parts of M87 ($r > 200$ kpc) is also well represented by the collisionless NFW profile with a mass of $M^{\rm M87} = 1.3 \times 10^{14}\, M_\odot$ and a concentration value of $c = 7$. This allows us to infer the M87 original DM profile by extrapolating $M^{\rm M87}_{\rm NFW}(r)$ down to $r = 0$ so that, defining $X \equiv r/R_{\rm vir}$, we have

$$V_{\rm NFW}(X)^2 = G\, M_{200}/R_{\rm vir} \frac{1}{X} \frac{\ln(1 + cX) - \frac{cX}{1+cX}}{\ln(1+c) - \frac{c}{1+c}}, \quad (8)$$

with $M_{200} = 200\, 4/3\pi\, \rho_c\, R^3_{\rm vir}$ and $\rho_c = 1.0 \times 10^{-29}$ g cm^{-3}. Then, $M_{\rm NFW}(r) = G^{-1} V^2(XR_{\rm vir}) r$.

The primordial distribution of the M87 DM halo leads us to realize that a significant fraction of the dark mass, once inside the radius $R_{\rm dom}$,[7] has gone missing: $\simeq \Delta M^{\rm M87}_{\rm NFW}(R_{\rm dom}) = M^{\rm M87}_{\rm NFW}(R_{\rm dom}) - M(R_{\rm dom}) \sim 2 \times 10^9\, M_\odot$.

A very relevant feature of the mass distribution of M87 is its huge DM core radius r_0; this is one of the first detections of DM cores as large as ~ 100 kpc (see also Di Paolo et al. 2019). Such a bare fact was also found by Oldham & Auger (2016a), although their result could be affected by the various biases of the density profiles adopted.

M87 has its say also in the most intriguing relationship of disk galaxies, i.e., that between the DM core radius r_0 and the disk length scale (Donato & Salucci 2004) R_D we realize (Salucci 2019) that it also holds in this giant galaxy (see Figure 4). In detail, we have that

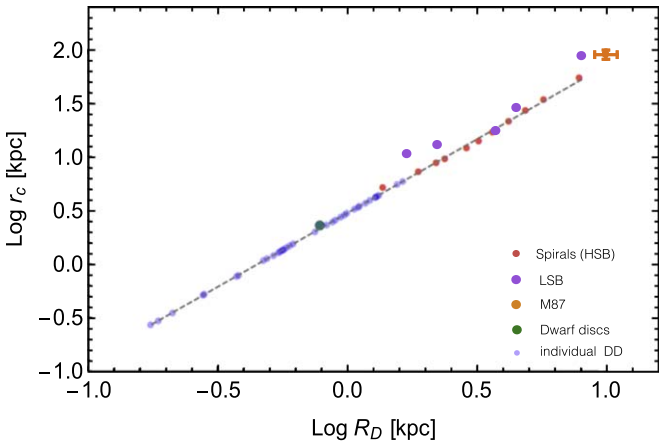

Figure 4. The core radius vs. disk scale length relationship in galaxies (see Salucci 2019 and references therein). M87 is represented given by the orange filled circle. It is noteworthy that the evidence of core radii ranges from 250 pc to 90 kpc.

$$R_D \equiv \frac{d \log \Sigma_\star}{d \log r}$$

(see Equation (1)), a quantity deeply connected with the luminous world that strongly correlates with

$$r_0 \equiv \frac{d \log \rho_h}{d \log r}|_{r=0}$$

a quantity that is, instead, deeply connected with the dark world. Remarkably the connection is at the level of the derivatives of corresponding densities.

Donato et al. (2009) discovered that, in all spirals, the central DM surface density $\Sigma_0 \equiv \rho_0 r_0$ is about constant, $\Sigma_0 \sim 120^{+200}_{-70}\, M_\odot$ pc^{-2}, independent of the galaxy magnitude. Such a relationship has been later confirmed across a range of 18 magnitudes (maximum circular velocity) and in galaxies of different Hubble types: dwarf spheroidal, dwarf irregulars, and LSBs (Salucci et al. 2012) (see also Salucci 2019). We realize that M87 follows such a relationship between dark world—dark world quantities within a factor 4. Furthermore, M87, with a stellar mass much higher than any other galaxy, is pivotal in indicating that in the above relationship, stellar mass also plays a role. A more accurate relationship involving two quantities of the DM component, ρ_0 and r_0, and one quantity of the luminous matter component $M_{\rm sph}$, emerges (Σ_0 in $M_\odot\, pc^{-2}$):

$$\log\, \Sigma_0 = 2.72 + \frac{1}{6} \log\left(\frac{M_{\rm sph}}{10^{12}\, M_\odot}\right), \quad (9)$$

with the scatter less of 0.15 dex.

3. The Central Supermassive Black Hole as a Mass Component of M87

The accurate mass model of M87 (see Section 2) and the very precise EHT determination of the mass of its SMBH (Akiyama et al. 2019a, 2019b) allow us to investigate the region in which the latter dominates the galaxy gravitational potential. First, we notice that, compared with other spheroidals, the fraction between the SMBH mass and the total stellar mass is quite high: 6×10^{-3}, especially considering that most of the $1.2 \times 10^{12}\, M_\odot$ of the M87 stellar spheroid has been accumulated at times much later than

[7] $R_{\rm dom}$ defines the region in which today the SMBH dominates the dynamics of M87, i.e., $R_{\rm dom}$=1 kpc (see Figure 3).

that of the formation of the SMBH. Using the full M87 mass model, we can derive the analogous circular velocity $V(r)$ from $r \sim 0.1$ kpc outwards, determining the various luminous, black hole, and dark matter components. Let us stress that, in the region $0.1\,\mathrm{kpc} < r < 10\,\mathrm{kpc}$, we recover $V(r)$ without having in this region dynamical measurements. The DM component here is negligible. The EHT independently measured the mass of the SMBH. Finally, this region's stellar mass distribution is obtained through high-resolution photometry alongside dynamical measurements at 10–30 kpc, where the stellar spheroids are the major massive component.

In Figure 3 we plot such curve out to 4 kpc; we realize that inside 1 kpc, the SMBH component dominates that of the stellar halo and, therefore, the whole gravitational potential. Remarkably, such a component gives an important contribution to the total velocity out to $4\,\mathrm{kpc} \simeq 0.4\,R_D$. This result is amazing: in late spirals, of any mass, the radius of the dominance of the SMBH is lesser than 20–50 pc $\sim 0.05\,R_D$ (Salucci et al. 2000). In elliptical galaxies, we do not see a dynamically dominant SMBH component in that the SMBHs with masses of $10^{8-9}\,M_\odot$ are buried inside stellar spheroids with a mass of $>10^{11}\,M_\odot$ within r_e.[8] To our knowledge, M87 is the unique object in which we can see the central black hole participating, with another mass component, in shaping the mass distribution of a galaxy. The two components, actually, look fine tuned, and the circular velocity of M87 keeps constant from 0.4 kpc to 4 kpc in spite of the fact that the components, in such region, have totally different velocity radial profiles: $V_{\rm SMBH}(r) \propto r^{-1/2}$ which contrasts $V_\star(r) \propto r^{1/2}$.

Another peculiar feature seems present in this region: a mysterious lack of DM. In fact, inside $0.1\,R_D = 1$ kpc the extrapolated back dark mass $M^{\rm M87}_{\rm NFW}(1\,\mathrm{kpc})$ is only 0.1% of $M\,(1\,\mathrm{kpc})$, computed from the M87* black hole mass and from accurate photometry and the mass-to-light ratio of the stellar spheroid. Inside R_D, where we have dynamical measurements of the total mass, the dark mass is 13% of $M(R_D)$. Only at $r > 22$ kpc does the dark matter contribution to the circular velocity overcome that of the standard matter.

In spheroidals the well-known $M_{\rm BH}$ versus $\log\,\sigma_e$ relationship is a fundamental one, e.g., Kormendy & Ho 2013):

$$\log \frac{M_{\rm BH}}{10^9\,M_\odot} = -0.51 \pm 0.05 + (4.4 \pm 0.03)\log \frac{\sigma_e}{200\ \mathrm{km\ s^{-1}}}. \quad (10)$$

Since in M87 $M_{\rm BH} = 6.5 \times 10^9\,M_\odot$ and $\sigma_e \simeq (358 \pm 5)\,\mathrm{km\,s^{-1}}$, the EHT SMBH mass results (0.2 ± 0.04) dex larger than the value predicted by Equation (10), showing a 5σ excess. Such excess, in mass (at 1σ) is of the order of $(3\text{–}4.5) \times 10^9\,M_\odot$. This is an important result, given the exquisite EHT black hole mass estimate and the fact that the Kormendy & Ho (2013) relationship is very tight. In fact, in the crucial process of the black hole mass growth, this result points to a role for the dark matter. This may be the first case in which one can argue that the DM component also contributed to the SMBH mass growth.

4. Discussion and Conclusions

For several issues of cosmology and extragalactic astrophysics, the determination of the M87 dark and standard matter mass distributions of this work becomes a phenomenal testbed and yields pivotal information. M87 is a giant cD galaxy of a total mass of $1.3 \times 10^{14}\,M_\odot$ which has, at its center, the usual SMBH, whose mass has been exquisitely measured in the process of imaging its shadow. In addition, we have an accurate mass distribution from 100 pc to 1 Mpc obtained by exploiting high-quality photometric and spectroscopic measurements.

Remarkably, the M87* SMBH, almost uniquely in the local universe, controls gravitationally a region $\simeq 1$ kpc wide, populated by more than 10^7 stars of the stellar spheroid. In contrast, in our Galaxy, the central SMBH hole Sgr A* dictates the motion of only a few thousand stars.

There is evidence that, inside $R_{\rm dom} \simeq 1$ kpc, a relevant portion of the original DM halo mass has disappeared over the Hubble time, in fact: $M_{\rm DM}(R_{\rm dom}, z_{\rm form}) - M_{\rm NFW}(R_{\rm dom}, 0) \sim 2 \times 10^9 M_\odot$. On the other side, the EHT estimate of the M87* mass results bigger, by approximately the same amount, than the value expected from the well-known $M_{\rm SMBH}$ versus $Log\ \sigma_e$ diagram, that people think is born out of an Eddington accretion of standard matter onto an SMBH seed. The following argument also supports the presence of a dark infall on M87*. In the case of a dark halo around an SMBH of $\sim 7 \times 10^9\,M_\odot$ whose density at $r = R_{\rm dom}$ is $\rho_{\rm DM} R_{\rm dom}$ as found in Section 3 develops for $r < R_{\rm dom}$ a cusp so that $\rho_{DMcusp}(r) = \rho_{\rm DM} R_{\rm dom}\,(r/R_{\rm DM})^{-2.5}$. The mass inside this hypothetical cusp will be 2×10^{11}, totally incompatible with the DM mass dynamically estimated at 20 kpc.

These features may lead to the first observed case in which one can argue that the DM component also contributed to the SMBH mass growth. More generally, one can envisage that inside the innermost hundreds of parsecs, the escape velocity from the giant black hole is much bigger than the dispersion velocity of the primordial dark matter halo particles. On this note, it is known that the capture of DM particles by the central black hole is a well-studied physical process (see, e.g., Gammaldi et al. 2016). Furthermore, let us recall that the energy and angular momentum of the DM particles in the innermost kiloparsec can be removed by the noncollisional status of the particles themselves: e.g., in the scenario of self-interacting dark matter particles and in that of interacting dark matter standard model particles (e.g., Salucci et al. 2020).

The SMBH seems to have been, over the cosmological times, dynamically "alive" in a surprising way: a "fine tuning" between the mass of M87* SMBH and the mass distribution of its stellar spheroid appears. In fact, in the region inside 4 kpc the effective circular velocity keeps constant, despite the stellar spheroid and the SMBH components having very different radial profiles and total masses. We can argue that the central SMBH has dynamically shaped the innermost portion of the stellar spheroid.

The $1 \times 10^{14}\,M_\odot$ massive M87 DM halo density is well reproduced by a Burkert profile with a $\sim$100 kpc wide core radius. Outside the region in which the dark halo coexists with the stellar spheroid, $r > 200$ kpc, the DM density converges to the NFW profile characteristic of the collisionless DM regime, as it occurs in spirals (Salucci 2019).

M87 is a benchmark for the idea that supernovae (SN) induced baryonic feedbacks, by flattening the original cuspy distribution, are the cause of the detected DM cores. The energy budget of this possible process can be easily computed. The (potential) energy $E_{\rm cf}$ is involved in the core-forming process, taking into account that, inside r_0, $\rho^{\rm M87}_{\rm NFW}(r) \gg \rho^{\rm M87}_{\rm DM}(r)$ is $E_{\rm cf} \sim 10^{62}$ erg. The stellar mass inside r_0 is about $\sim 8 \times 10^{11} M_\odot$ which implies, for a single

[8] Of course, the accretion disk maser sources are totally subject to the SMBH gravitational field.

burst of star formation with a Salpeter initial mass function, the explosions of $\sim 5 \times 10^9$ core-collapse SNe, which in turn provide the energy of $f_{\rm cf} 10^{51}$ erg to the core-forming process, where $f_{\rm cf} \sim 10^{-1}$–10^{-2}. The cumulative feedback energy, therefore, does not reach 10^{60} erg $\ll E_{\rm cf}$. Notice that also in the biggest spirals the SN feedback is short of providing sufficient energy, but in M87 the failure is outstanding.

The stellar spheroid and the DM halo main structural length scales, $R_D^{\rm M87}$ and r_0, already mysteriously related in disk systems of any mass and morphology (Salucci 2019; Salucci et al. 2020), continue to be clone-like entangled also in this extremely different galaxy.

The M87 DM structural properties give decisive results in one important test about the nature of the dark particles. A preferred solution for the riddle of the observed cored DM distributions around galaxies involves the role of the fuzzy dark matter (FDM), a hypothetical particle (e.g., an ultra-light axion) with a mass of the order of $m_p = 10^{-22}$ eV that implies a de Broglie wavelength on the galaxy scales. FDM halos well reproduce the kinematics of dwarf galaxies with halo masses $M_h \sim 10^{9-10} M_\odot$ (e.g., Schive et al. 2014; Hui et al. 2017; de Martino et al. 2020; Pozo et al. 2021, and references therein). At larger masses the situation is completely open. However, in combination with the recent result by Burkert (2020) according to which Σ_0, r_0, and the galaxy redshifts of halo formation $z_{\rm form}$ are related by

$$\frac{r_0^3}{\rm kpc^3} = 0.25(1 + z_{\rm form}) \frac{75\ M_\odot pc^{-2}}{\Sigma_0} \frac{10^{-22}{\rm eV}}{m_p} \qquad (11)$$

the present result draws light on an important feature. For our galaxy, of mass $M_{200}^{\rm M87} = 1.3 \times 10^{14}\ M_\odot$, we have $z_{\rm form} < 5$, $\Sigma_0 \sim 500\ M_\odot\ {\rm pc}^{-2}$ and $r_0 \sim 90$ kpc, then Equation (11) holds only for particle masses whose de Broglie wavelengths are at the level of a megaparsec scale and are therefore unable to account for the DM halo density cores. Considering the family of normal spirals, Burkert (2020) noticed the implausibility, in the current galaxy formation theory, of the $r_0 \propto (1 + z_{\rm form})^{1/3}$ relationship in Equation (11). Overall, in M87 we conclude that the inferred value of r_0 gives results totally inconsistent with the prediction of Equation (11): the latter cannot be claimed to dictate the size of the constant-density region in galaxies.

M87 provides evidence that the primordial DM halo distribution has been modified by the combined action of the central SMBH and the stellar spheroid during the entire life of the universe. Therefore, it could be the place in which a new paradigm for the dark matter phenomenon arises: the latter's nature will emerge by reverse engineering the entanglement among the dark–luminous structural properties that we detect in galaxies rather than coming from theoretical first principles.

ORCID iDs

Mariafelicia De Laurentis https://orcid.org/0000-0002-9945-682X
Paolo Salucci https://orcid.org/0000-0002-9015-9722

References

Agnello, A., Evans, N. W., & Romanowsky, A. J. 2014, MNRAS, 442, 3284
Akiyama, K., Alberdi, A., Alef, W., et al. 2019a, ApJL, 875, L1
Akiyama, K., Alberdi, A., Alef, W., et al. 2019b, ApJL, 875, L6
Burkert, A. 2020, ApJ, 904, 161
de Blok, W. J. G. 2010, AdAst, 2010, 789293
de Martino, I., Chakrabarty, S. S., Cesare, V., et al. 2020, Univ, 6, 107
Dehghani, R., Salucci, P., & Ghaffarnejad, H. 2020, A&A, 643, A161
Di Cintio, A., Brook, C. B., Dutton, A. A., et al. 2014, MNRAS, 441, 2986
Di Paolo, C., Salucci, P., & Erkurt, A. 2019, MNRAS, 490, 5451
Donato, F., Gentile, G., Salucci, P., et al. 2009, MNRAS, 397, 1169
Donato, F., & Salucci, P. 2004, MNRAS, 353, L17
Freeman, K. 1970, ApJ, 160, 811
Gammaldi, V., Avila-Reese, V., Valenzuela, O., & Gonzales-Morales, A. X. 2016, PhRvD, 94, 121301
Gentile, G., Salucci, P., Klein, U., & Granato, G. L. 2007, MNRAS, 375, 199
Hui, L., Ostriker, J. P., Tremaine, S., & Witten, E. 2017, PhRvD, 95, 043541
Karukes, E. V., & Salucci, P. 2016, MNRAS, 465, 4703
Klypin, A., Kravtsov, A. V., Bullock, J. S., & Primack, J. R. 2001, ApJ, 554, 903
Kormendy, J., & Ho, L. C. 2013, ARA&A, 51, 511
Murphy, J. D., Gebhardt, K., & Adams, J. J. 2011, ApJ, 729, 129
Napolitano, N. R., Pota, V., Romanowsky, A. J., et al. 2014, MNRAS, 439, 659
Navarro, J. F., Frenk, C. S., & White, S. D. M. 1996, ApJ, 462, 563
Oldham, L. J., & Auger, M. W. 2016, MNRAS, 457, 421
Oldham, L. J., & Auger, M. W. 2016a, MNRAS, 457, 421
Oldham, L. J., & Auger, M. W. 2016b, MNRAS, 455, 820
Persic, M., Salucci, P., & Stel, F. 1996, MNRAS, 281, 27
Pozo, A., Broadhurst, T., De Martino, I., et al. 2021, MNRAS, 504, 2868
Salucci, P. 2007, in Dark Galaxies and Lost Baryons, Proc. of the IAU 244 (Cambridge: Cambridge Univ. Press), 53
Salucci, P. 2018, FoPh, 48, 1517
Salucci, P. 2019, A&ARv, 27, 2
Salucci, P., Lapi, A., Tonini, C., et al. 2007, MNRAS, 378, 41
Salucci, P., Ratnam, C., Monaco, P., & Danese, L. 2000, MNRAS, 317, 488
Salucci, P., Turini, N., & Di Paolo, C. 2020, Univ, 6, 118
Salucci, P., Wilkinson, M. I., Walker, M. G., et al. 2012, MNRAS, 420, 2034
Salucci, P., Esposito, G., Lambiase, G., et al. 2021, FrP, 8, 603190
Schive, H.-Y., Liao, M.-H., Woo, T.-P., et al. 2014, PhRvL, 113, 261302
Schuberth, Y., Richtler, T., Hilker, M., et al. 2010, A&A, 513, A52
Strader, J., Romanowsky, A., Brodie, J., et al. 2011, ApJS, 197, 33
Walsh, J. L., Barth, A. J., Ho, L. C., & Sarzi, M. 2013, ApJ, 770, 86
Zhu, L., Long, R. J., Mao, S., et al. 2014, ApJ, 792, 59